Modern Pathology (2014) 27, 1088–1100

A novel hypoxia-associated subset of FN1^{high}MITF^{low} melanoma cells: identification, characterization, and prognostic value

Jasper Wouters[1], Marguerite Stas[2], Olivier Govaere[1], Kathleen Barrette[3], Aleksandra Dudek[4], Hugo Vankelecom[5], Lauren E Haydu[6,7], John F Thompson[6], Richard A Scolyer[6,8] and Joost J van den Oord[1]

[1]Translational Cell and Tissue Research, Department of Imaging and Pathology, University of Leuven (KU Leuven), Leuven, Belgium; [2]Surgical Oncology, Department of Oncology, University of Leuven (KU Leuven), Leuven, Belgium; [3]Laboratory of Dermatology, Department of Oncology, University of Leuven (KU Leuven), Leuven, Belgium; [4]Laboratory of Cell Death Research and Therapy, Department of Cellular and Molecular Medicine, University of Leuven (KU Leuven), Leuven, Belgium; [5]Embryo and Stem Cells, Department of Development and Regeneration, University of Leuven (KU Leuven), Leuven, Belgium; [6]Melanoma Institute Australia, University of Sydney, Sydney, NSW, Australia; [7]Discipline of Surgery, Sydney Medical School, University of Sydney, Sydney, NSW, Australia and [8]Tissue Pathology and Diagnostic Oncology, Royal Prince Alfred Hospital, Camperdown, Sydney, NSW, Australia

In many human cancers, the epithelial-to-mesenchymal transition has an important role in the induction of cancer stem-like cells, and hence, in the causation of intratumoral heterogeneity. This process, also referred to as mesenchymal mimicry, is, however, only poorly understood in melanoma and histological correlation is still lacking. In an immunohistochemical analysis of a large prospective series of 220 primary and metastatic melanomas for the well-known epithelial-to-mesenchymal transition marker FN1, we observed melanoma cells with high FN1 expression in metastases with ischemic necrosis, but rarely or not at all in samples lacking evidence of hypoxia. In a blinded, retrospective series of 82 melanoma metastases with 10-year follow-up, the presence of clusters of these FN1^{high} melanoma cells correlated significantly with shortened melanoma-specific survival, highlighting the prognostic value of their presence. We describe in detail the unique light- and electron-microscopic features of these FN1^{high} melanoma cells, enabling their identification in routinely hematoxylin-and-eosin-stained sections. In addition, by laser microdissection and subsequent gene expression analysis and immunohistochemistry, we highlight their distinctive, molecular phenotype that includes expression of various markers of the epithelial-to-mesenchymal transition (eg, ZEB1) and of melanoma stem-like cells (eg, NGFR), and lack of immunoreactivity for the melanocytic marker MITF. This phenotype could be reproduced *in vitro* by culturing melanoma cells under hypoxic conditions. Functionally, the hypoxic microenvironment was shown to induce a more migratory and invasive cell type. In conclusion, we identified a novel clinically relevant FN1^{high}MITF^{low} cell type in melanoma associated with ischemic necrosis, and propose that these cells reside at the crossroad of the epithelial-to-mesenchymal transition and stem-like cell induction, plausibly triggered by the hypoxic environment.

Modern Pathology (2014) **27,** 1088–1100; doi:10.1038/modpathol.2013.228; published online 3 January 2014

Keywords: fibronectin (FN1); epithelial-to-mesenchymal transition; melanoma; microphthalmia-associated transcription factor (MITF); stem-like cancer cell

Cutaneous melanoma is notorious for its heterogeneity, both at morphologic and phenotypic levels.[1,2] In contrast to the homogeneous appearance of *in vitro* melanoma cell lines, the remarkable heterogeneity of *in vivo* cutaneous melanoma suggests an important role of the tumor microenvironment in determining the morphology and phenotype and, consequently, the function of

Correspondence: Bio-Ir J Wouters, MSc, PhD, Translational Cell and Tissue Research, Department of Imaging and Pathology, University of Leuven (KU Leuven), Minderbroedersstraat 12 blok q—box 1032, B-3000, Leuven, Belgium.
E-mail: jasper.wouters@med.kuleuven.be
Received 24 July 2013; accepted 22 October 2013; published online 3 January 2014

subsets of melanoma cells.[3] As in other cancers, this heterogeneity in melanoma may be driven by a small subpopulation of 'stem-like' melanoma cells that gives rise to a morphologically and phenotypically diverse progeny.[4,5] According to the phenotype switch model in melanoma,[6] it has been suggested that, in response to soluble mediators released by stromal cells in the tumor microenvironment, melanoma cells can switch between a quiescent subtype of motile, invasive cells and a proliferative, more 'differentiated' tumor cell type; the former subset would contribute to metastasis and carry a phenotype closely related to the stem cell-like status, whereas the latter subset would contribute to tumor mass and carry a more differentiated phenotype. Hence, 'stemness' in melanoma would be a temporary status dictated by environmental factors rather than a well-established, permanent feature.[6]

The invasive subset of neoplastic cells, closely related to the stem cell-like subset, is characterized by a fibroblast-like morphology, loss of adhesion receptors, enhanced motility, and invasiveness and by the acquisition of additional mesenchymal features such as expression of VIM and FN1 as a result of epithelial-to-mesenchymal transition, also referred to as mesenchymal mimicry.[7] Although originally described for epithelial cells and epithelial cancers, the epithelial-to-mesenchymal transition also affects non-epithelial cells such as melanocytes and associated tumors.[8] High-throughput analyses in cutaneous melanoma have indeed identified the epithelial-to-mesenchymal transition as a major determinant of metastasis.[9] In addition, expression of the well-established epithelial-to-mesenchymal transition marker FN1[7] has been reported to be upregulated in melanomas *versus* benign nevi[10,11] as well as in melanoma metastases *versus* primary melanomas.[12]

To date, the above-mentioned functional subsets of melanoma cells cannot be discerned within the heterogeneous population of melanoma cells using routine histology. By immunohistochemical analysis of a large prospective series of 220 primary and metastatic melanomas for the epithelial-to-mesenchymal transition marker FN1, we observed a distinct subset of melanoma cells displaying high FN1 expression. These cells were predominantly seen in melanoma metastases with signs of tumor necrosis. In addition, in a blinded retrospective series of melanomas with 10 years follow-up, their presence correlated with reduced melanoma-specific survival. We describe their unique morphological characteristics to enable their identification/recognition in routinely stained sections. We further characterized the molecular phenotype of microdissected FN1^{high}MITF^{low} by gene expression analysis and immunohistochemistry, and provide evidence for their importance in cell migration/invasion, and for their relation with hypoxia.

Materials and methods

Melanoma Specimens

Melanoma samples were obtained after surgical resection in the University Hospital Leuven (Belgium) and used in this study as approved by the local Ethical Committee. Part of the tumor was fixed in buffered formalin and embedded in paraffin for routine histology and immunohistochemistry; and part was snap-frozen in liquid nitrogen-cooled isopentane. For prospective analyses, all primary melanomas and metastases between May 2011 and December 2012 were used and studied as described below. For retrospective analyses, archival formalin-fixed, paraffin-embedded metastatic melanoma specimens were obtained from patients with >10 years of clinical follow-up treated at Melanoma Institute Australia with IRB approval (Sydney South West Area Health Service Institutional Ethics Review Committee (RPAH Zone) Protocols: No. X08-0155/HREC 08/RPAH/262, No. X11-0023/HREC 11/RPAH/32 and X07-0202/HREC/07/RPAH/30). A cohort of patients was identified from the Melanoma Institute Australia research database that initially presented with clinically metastatic lymph nodes and was managed with therapeutic lymph node dissection. Patients with concurrent in-transit or distant metastases were excluded. From this overall cohort ($n=551$), available lymph node tissue specimens ($n=82$) were selected and studied for clinical significance of FN1^{high} melanoma cells. Tumors were subjected to further analysis as described below.

All melanocytic lesions were stained with hematoxylin and eosin (H&E) for routine diagnosis, and by immunohistochemistry for MITF (as a negative marker) and FN1 (as a positive marker) on serial sections.

Melanoma Cell Culture

The human melanoma cell line A375[13] was cultured in Dulbecco's modified Eagle's medium/Ham's F12 (Lonza, Verviers, Belgium) supplemented with 10% fetal bovine serum (Lonza), antibiotic/antimycotic (Life Technologies, Ghent, Belgium), and 4 mM L-glutamine (Life Technologies). Cell cultures were regularly tested for mycoplasma contamination by PCR, and were found negative (data not shown). For the analyses described below, cells were released from the culture vessel and dissociated into single cells using trypsin (0.05%) with EDTA (Life Technologies). To investigate the effect of hypoxia, A375 cells were cultured in 1.5% O_2/5% CO_2 ('*In Vivo*2 400' hypoxic incubator; Ruskinn Technology, Bridgend, UK) and compared with A375 cells cultured under standard cell-culture conditions (20% O_2/5% CO_2).

Transmission Electron Microscopy

For transmission electron microscopy, frozen samples from two melanoma metastases with large

numbers of FN1^{high} cells and from one melanoma metastasis without such cells were used. Frozen H&E-stained sections were used to select representative areas; subsequently, these small areas were punched out of the frozen samples and thawed in 2.5% glutaraldehyde, post-fixed in OsO_4 and embedded in Epon for transmission electron microscopy.

Immunohistochemistry/Immunocytochemistry

Immunohistochemistry for melanocytic, stromal, and various other proteins, listed in Supplementary Table 1, was performed on paraffin-embedded or frozen material of primary and metastatic melanomas, using well-characterized primary antibodies and the indirect EnVision FLEX system (Dako, Heverlee, Belgium). Antigen retrieval was performed in a pre-treatment module (Dako) according to the manufacturer's instructions in citrate buffer at pH 6 or in EDTA-Tris buffer, pH 9 (Supplementary Table 1). Peroxidase activity was detected using 3,3′-diaminobenzidine as substrate, revealing a brown reaction product in unpigmented lesions, or 3-amino-9-ethylcarbazole, revealing a red reaction product in heavily pigmented lesions. Double immunohistochemical staining was performed with a sequential technique[14] using primary antibodies raised in different species, and sequential development of peroxidase and alkaline phosphatase with 3,3′-diaminobenzidine and Bond Polymer Refine Red Detection (Leica Microsystems, Wetzlar, Germany), respectively, resulting in contrasting dark brown and pink/red immunoreactivities. A375 melanoma cells exposed to hypoxic conditions, and controls, were fixed in acetone at $-20\,^{\circ}C$ for 10 min, followed by standard immunohistochemistry.

Scoring of Retrospective, Clinical Cohort

Tissue samples were randomized and coded for technicians and researchers. H&E staining and FN1 immunohistochemistry were scored semi-quantitatively and independently by two blinded researchers (negative, no FN1^{high} melanoma cells; low, scattered FN1^{high} melanoma cells; medium, few clusters of FN1^{high} melanoma cells; high, abundant clusters of FN1^{high} melanoma cells; clusters were defined as cohesive groups of at least 10 cells in diameter with the morphological features, outlined above, and/or with cytoplasmic expression of FN1; see Supplementary Figure 1 for representative slides; see Supplementary Table 2 for cohort characteristics). Melanoma-specific survival was defined as the interval from therapeutic lymph node dissection to death from melanoma or date of last follow-up. Melanoma-specific survival was assessed using the Kaplan–Meier method together with the Log-Rank (Mantel–Cox) test for significant comparisons of FN1 expression.

Laser Capture Microdissection

Cryosections (10 μm thick) were cut and mounted onto ultraviolet-treated PET-membrane-coated metal frame slides (1.4 μm; Leica Microsystems). Samples were fixed in cold acetone for 10 min, stained with rabbit anti-FN1 antibody for 5 min and Alexa Fluor 568 goat anti-rabbit antibody for 1 min (Supplementary Table 1), and dehydrated in consecutive washes of 75 and 95% ethanol for 30 s each, and for 2 min in 100% ethanol. FN1^{positive} and FN1$^{low/negative}$ melanoma cells were identified and selected based on their morphology (H&E on an adjacent tissue section) and on FN1 immunostaining. Selected groups of cells were microdissected using a Leica DM6000B (Leica Microsystems). Isolated fragments were captured on the cap of AdhesiveCap 500 Opaque tubes (Carl Zeiss, Zaventem, Belgium) and were snap frozen in dry ice and stored at $80\,^{\circ}C$ until further processing.

RNA Extraction, cDNA Synthesis, and qPCR

RNA samples from frozen tissue sections were prepared using the TRIzol/chloroform phase separation. RNA quality and concentrations were measured with a Nanodrop 1000 spectrophotometer (Thermo Scientific, Erembodegem, Belgium). First-strand cDNA was produced with the M-MLV reverse transcriptase (Invitrogen/Life Technologies) and random hexamer primers (Fermentas/Thermo Scientific), according to the manufacturer's protocol. Total RNA from A375 melanoma cells exposed to hypoxic conditions, and controls, was extracted using the RNeasy Mini Kit (Qiagen, Venlo, the Netherlands) according to the manufacturer's protocol (including DNase treatment), and quality and concentration determined with a Nanodrop 1000 spectrophotometer (Thermo Scientific). cDNA was constructed with the iScript cDNA kit (Bio-Rad, Nazareth Eke, Belgium). Quantitative RT-PCR was carried out as described previously,[15] using Fast SYBR Green Master Mix (Applied Biosystems/Life Technologies) on an ABI 7900HT Fast PCR system according to the manufacturer's protocol. Oligonucleotide primers for qPCR (Supplementary Table 1) were designed with Perlprimer[16] unless stated otherwise and validated for comparable amplification efficiency (data not shown). Samples for quantitative PCR were assayed in duplicate. Negative controls and dissociation curves were used to confirm specific amplification. Normalized, relative expression data were calculated using the comparative threshold cycle (2ddCt) method.[17]

Western Blot

Cells were lysed using lysis buffer (25 mM HEPES, 0.3 mM NaCl, 1.5 mM $MgCl_2$, 20 mM β-glycerolphosphate, 2 mM EDTA, and 2 mM EGTA (pH 7.5))

containing 1% Triton, 10% glycerol, 1 mM Na_3VO_4, 0.5 mM dithiothreitol, 10 μg/ml leupeptin, 10 μg/ml aprotinin, and 10 μg/ml antipain and phosphatase inhibitor cocktail (phosSTOP; Roche, Vilvoorde, Belgium). Protein concentration was determined using the BCA Protein Assay Reagent (Thermo Scientific). Equal amounts of protein from each sample were separated by electrophoresis through SDS-PAGE gels (Invitrogen/Life Technologies), transferred to a nitrocellulose membrane (Whatman Protran, Kent, UK) and analyzed by immunoblotting. Equal loading of proteins was verified using Ponceau-S (see Supplementary Table 1 for primary antibodies). Protein bands were visualized using enhanced chemiluminescence as described by the supplier (GE Healthcare Life Sciences, Diegem, Belgium) and quantified from digitized photographs using UN-SCAN-IT software (Un-scan-it, Silk Scientific, Orem, UT, USA).

Proliferation Assay

Mitotic index was assessed by immunohistochemistry for pHH3.[18] Briefly, cells were plated and grown in normoxic/hypoxic conditions for 3 days. Three to six optical fields ($\times$ 10 magnification) were randomly chosen and cells were counted. In parallel, immunohistochemistry for pHH3 was performed on fixed cells and analyzed. Both analyses were done using NIH Image J software.[19]

Migration Assay

Cell migration was assessed by an *in vitro* wound-healing scratch assay as previously described.[20] Briefly, cells were plated and grown in normoxic/hypoxic conditions for 3 days (triplicate). A scratch was made in the near-confluent cell layer using a P200 plastic tip (time point 0). Cells were washed once with growth medium to remove residual cell debris, and medium was replaced with low-serum (2%) growth medium to minimize cell proliferation.[20] After 16 h in normoxic/hypoxic conditions, the migrated surface area was quantified using the TScratch software and normalized to time point 0.[21]

Invasion Assay

The invasive potential of cells grown in normoxic/hypoxic conditions for 3 days was examined using QCM ECMatrix Cell Invasion Assay, a 24-well plate (8 μm), colorimetric (Millipore, Billerica, MA, USA; triplicate) according to the manufacturer's instructions. Briefly, single cells (3×10^5 cells/chamber) were cultured in serum-free growth medium in normoxic/hypoxic conditions. Heat-inactivated fetal bovine serum (10%) was used as a chemoattractant. After 24 h, invaded cells were visualized with crystal violet stain and quantified by manual counting and with an UV Max Kinetic Microplate reader (Molecular Devices, Sunnyvale CA, USA) at an optical density of 560 nm.

Statistics

Log-Rank (Mantel–Cox) test of melanoma-specific survival was carried out with SAS version 9.3 (Cary, NC, USA). All other data were analyzed using the two-tailed Student's *t*-tests with Graphpad Prism 5.02 (GraphPad Software, La Jolla, CA, USA).

Results

Incidence, Morphology, and Clinical Significance of FN1^{high} Cells in Cutaneous Melanoma

We performed an immunohistochemical analysis for the epithelial-to-mesenchymal transition marker FN1 in a prospective series of 92 primary cutaneous melanomas and 128 metastatic melanomas. The metastases comprised 62 lymph node metastases (20 axillary, 9 cervical, 18 inguinal, 8 iliacal, 2 plopliteal, and 5 from unknown origin), 36 visceral metastases (20 (sub)cutaneous, 4 intestinal, 4 lung, 4 brain, 2 breast, 2 stomach), and 30 cutaneous in-transit metastases. In addition to the expected expression in the stroma, melanoma cells displaying a distinct intracellular FN1 staining were detected (Figure 1a). These FN1^{high} melanoma cells were observed in 32/128 metastases; the majority (30/32) of these metastases showed variably sized areas of ischemic tumor necrosis. In contrast, this cell type was only observed in 2/92 primary melanomas, all of which lacked signs of necrosis, and in 2/32 metastatic melanomas lacking necrosis. Of the 96 metastatic melanomas lacking FN1^{high} melanoma cells, 28 showed variably sized areas of necrosis.

In H&E-stained sections, FN1^{high} melanoma cells could be distinguished from the main tumor cell population by their small size, flattened or angulated, often indented hyperchromatic nucleus and scarce eosinophilic cytoplasm in light microscopy; nucleoli were conspicuously absent (Figure 1b). FN1^{high} melanoma cells were found either scattered as single cells or in small collections with their nuclei often oriented parallel to each other (Figures 1a–e). FN1^{high} melanoma cells were predominantly located at the border of, or within fibrovascular septa but did not form discernible vessels. They were not observed at the border of necrotic tumor areas (Figure 1b) where early necrotic melanoma cells with rounded nuclear shape were distinctly different from the small FN1^{high} melanoma cells away from areas of necrosis. In transmission electron microscopy of an area rich in FN1^{high} melanoma cells, small melanoma cells with high nucleo-cytoplasmic ratio and distinctive nuclear morphology, ie, prominent heterochromatin and lack of nucleoli, could be recognized. In the

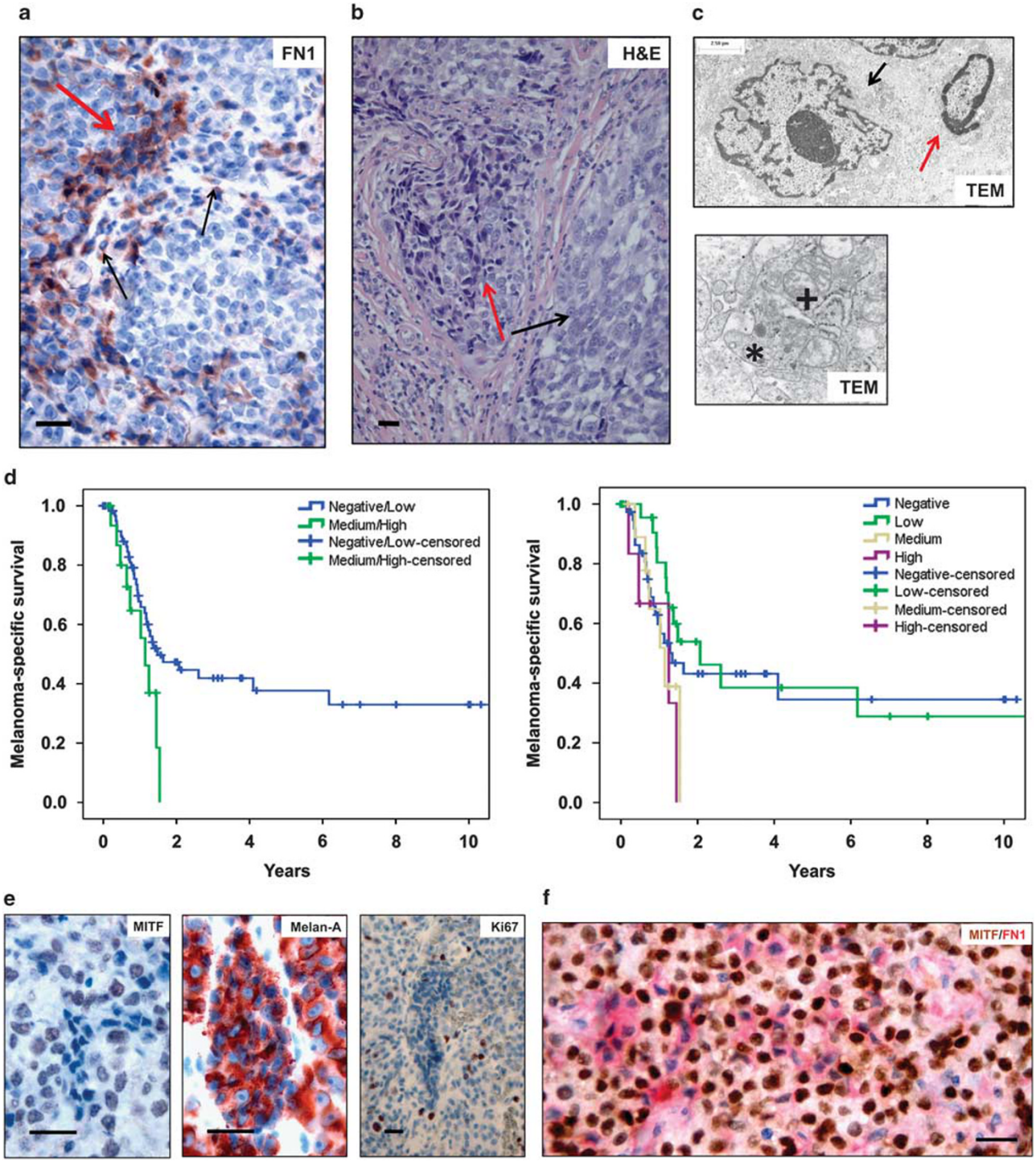

Figure 1 Morphology, clinical significance, and immunohistochemical profile of FN1^{high} cells in human melanoma. (**a**) Immunohistochemical staining showing FN1 expression in stromal cells and intracellular FN1 expression in melanoma cells (scale bar, 75 μm; black arrows, stromal FN1 expression; red arrow, intracellular FN1 expression in melanoma cells). (**b**) Hematoxylin-and-eosin-stained section displaying FN1^{high} melanoma cells as small cells with eosinophylic cytoplasm and a flattened or angulated hyperchromatic nucleus (scale bar, 75 μm; black arrow, normal melanoma cells; red arrow, FN1^{high} melanoma cells). (**c**) Transmission electron microscopy demonstrating prominent heterochromatin, lack of nucleoli, immature mitochondria, and melanosomes in FN1^{high} cells (scale bars, 2.5 and 0.25 μm, respectively; black arrow, normal melanoma cell; red arrow, FN1^{high} melanoma cell; +, mitochondrion; *, melanosome). (**d**) Kaplan–Meier curve showing the cumulative survival of patients with metastatic melanomas with various numbers of FN1^{high} melanoma cells ($n=82$; negative, no FN1^{high} melanoma cells; low, scattered FN1^{high} melanoma cells; medium, few clusters of FN1^{high} melanoma cells; high, abundant clusters of FN1^{high} melanoma cells; statistical significance was tested with the Log-Rank (Mantel–Cox) test). (**e**) Immunohistochemical staining of melanoma sections showing FN1^{high} melanoma cells that express melan-A but lack MITF and Ki67 expression (scale bar, 75 μm). (**f**) Double immunostaining showing inverse correlation between FN1 and MITF immunoreactivity (scale bar, 75 μm; dark brown nuclear staining, MITF; pink/red cytoplasmic staining, FN1; blue nuclear staining, hematoxylin).

cytoplasm of these melanoma cells, melanosomes with an immature aspect were found (Figure 1c).[22] In the control sample taken from a melanoma metastasis without FN1^{high} melanoma cells, no such cells were discerned (data not shown).

The clinical significance of FN1^{high} melanoma cells was studied in a retrospective series of 82 melanoma metastases from patients with at least 10 years of clinical follow-up. H&E staining and FN1 immunohistochemistry were scored semi-quantitatively and independently by two blinded researchers (see Materials and methods). The scores from H&E staining and FN1 immunohistochemistry correlated significantly (Spearman $r=0.66$; $P<0.0001$), indicating the consistent light-microscopic morphological characteristics of FN1^{high} melanoma cells. Melanoma-specific survival gradually decreased from patients lacking FN1^{high} melanoma cells, over patients with scattered FN1^{high} melanoma cells, to patients with few and abundant clusters of FN1^{high} melanoma cells, respectively, although the result was not statistically significant ($P=0.184$; Figure 1d). Moreover, melanoma patients with clusters of FN1^{high} melanoma cells had a significantly shorter disease-specific survival compared with patients with at most scattered FN1^{high} melanoma cells ($P=0.044$; Figure 1d).

Immunohistochemical Profile of FN1^{high} Melanoma Cells

As FN1^{high} melanoma cells were predominantly observed in metastatic melanomas, their detailed immunophenotype was determined in a retrospective series of 17 metastatic melanomas in which distinctive clusters of FN1^{high} melanoma cells were observed (based on morphology in H&E staining and FN1 immunoreactivity). FN1^{high} melanoma cells displayed S100 immunoreactivity and positivity with variable intensity for melanoma markers such as Melan-A, HMB45, and TYR, whereas immunoreactivity for the melanocytic marker MITF was invariably weak or absent in contrast to the intense nuclear MITF positivity in adjacent large polygonal melanoma cells (Figure 1e and Supplementary Figure 2A; see Table 1 for a summary of immunohistochemical results). Hence, immunostaining for MITF easily identified the FN1^{high} melanoma cells by their flattened hyperchromatic blue (ie, not immunoreactive) nuclei. The inverse correlation between FN1 and MITF immunoreactivity was confirmed by double staining in seven MITF^{positive} metastases, in which FN1^{high} melanoma cells with pink/red-stained cytoplasm displayed a blue, unstained, or MITF^{low} nucleus upon hematoxylin counterstaining, contrasting with the vast majority of melanoma cells showing a dark brown (MITF^{high}) nuclear signal and unstained cytoplasm (Figure 1f). Moreover, FN1^{high} melanoma cells often displayed more intense immunoreactivity than FN1^{high} stromal cells in fibrovascular septa and than the overall staining in the extracellular matrix (Figure 1f and Supplementary Figure 2B).

Given their mesenchymal aspect (ie, flattened nucleus, elongated shape, and high FN1 expression), FN1^{high}MITF^{low} melanoma cells were further studied for various markers of stromal cells, ie, endothelium (CD31, CD34, D2-40 or podoplanin, CAV1, CD144), smooth muscle cells and myofibroblasts (alpha-SMA), dermal dendrocytes (coagulation factor XIIIa), leukocytes (CD45), and macrophages (CD68). All stromal markers were absent in FN1^{high}MITF^{low} melanoma cells (Supplementary Figure 2A).

Finally, FN1^{high}MITF^{low} melanoma cells were negative for proliferation-associated Ki67 immunoreactivity (Figure 1a), suggesting a quiescent state. Moreover, the cell type was neither associated with apoptosis nor with senescense, given their lack of cleaved CASP3 immunoreactivity and β-galactosidase activity, respectively (Supplementary Figure 2C).

Transcriptomic Analysis of FN1^{high} Melanoma Cells and Validation by Immunohistochemistry

Because of their immature and mesenchymal features, we hypothesized that FN1^{high}MITF^{low} melanoma cells may correspond, or be closely related, to the subset of melanoma cells in the stem cell-like status with migratory capacities because of the epithelial-to-mesenchymal transition, previously described by Hoek and Goding.[6] Therefore, we investigated whether FN1^{high}MITF^{low} melanoma cells express additional epithelial-to-mesenchymal transition markers as well as previously proposed stem-like melanoma cell markers (Supplementary Table 1). Following immunofluorescent staining of frozen sections of four cases of metastatic melanoma, cell clusters showing a FN1 signal and not representing stromal cells (based on analysis of an adjacent H&E-stained section) were microdissected from serially cut and stained sections and their gene expression analyzed by RT-qPCR. As a control, adjacent FN1$^{low/negative}$ melanoma cell clusters were sampled. RT-qPCR analysis revealed no significant differences in expression levels of melanocytic genes (*S100A6* and *TYR;* see Table 1 for a summary of RT-qPCR results) between FN1^{high} and FN1$^{low/negative}$ melanoma cells (Supplementary Figure 3). In contrast, FN1^{high} melanoma cells expressed significantly higher levels of *FN1*, *HIF2A* (or *EPAS1*), *NGFR,* (or *CD271*) and *ZEB1*, and significantly lower levels of *M-MITF* and *TWIST1* (Figure 2a). Three other factors, previously shown to be associated with the melanoma stem-like cell status (*ABCB5*, *JARID1B* or *KDM5B,* and *SNAI1*) displayed an upward trend in FN1^{high} melanoma cells, although not statistically significant (Figure 2a). Microdissected FN1^{high} and FN1$^{low/negative}$ melanoma cells showed no significant differences in mRNA levels of other proposed melanoma stem-like or epithelial-to-mesenchymal

Table 1 Gene and protein expression in FN1^{High} and FN1$^{Low/negative}$ melanoma cells

Gene	*FN1^{High} versus FN1$^{Low/negative}$ melanoma cells*[a]
ABCB5	+[b]
CD133	No expression
ETS1	0
FN1	+
HIF1A	0
HIF2A	+
JARID1B	+[b]
KLF4	0
M-MITF	−
NANOG	0
NES	0
NGFR	+
OCT4	0
S100A6	0
SNAI1	+[b]
SNAI2	0
TWIST1	−
TYR	0
ZEB1	+
ZEB2	0

Protein	*FN1^{High} melanoma cells*[c]	*FN1$^{Low/negative}$ melanoma cells*[c]
Beta-galactosidase	−	−
CAV1	−	−
CD133	−	−
CD144	−	−
CD31	−	−
CD34	−	−
CD45	−	−
CD68	−	−
Cleaved CASP3	−	−
Coagulation factor XIIIa	−	−
D2-40	−	−
FN1	+	−
HIF2A[d]	+	+
HMB45	+&	+
Ki67	−	+
Melan-A	+&	+
MITF	−	+
NES	−	−
S100	+	+
SMA	−	−
TYR	+&	+
ZEB1	+[e]	−

[a] +, Higher expression; −, lower expression; 0, similar expression.
[b] Non-significant.
[c] +, Expression; −, no expression; &, variable intensity.
[d] Higher intensity in FN1^{high}MITF^{low} melanoma cells than in other melanoma cells.
[e] A subset of FN1^{high}MITF^{low} melanoma cells.

transition markers such as *ETS1*, *HIF1A*, *KLF4*, *NANOG*, *NES*, *OCT4* (or *POU5F1*), *SNAI2,* and *ZEB2* (Supplementary Figure 3). Finally, *CD133* (or *PROM1*) gene expression was observed in neither FN1^{high} nor FN1$^{low/negative}$ melanoma cells (data not shown).

Gene-expression data were validated by immunohistochemistry for a selection of the genes. Immunoreactivity for TYR and FN1, and weak (or lack of) MITF expression were confirmed (see also Figures 1a–e). Although most melanoma cells showed cytoplasmic HIF2A expression, HIF2A immunoreactivity was markedly stronger in FN1^{high} MITF^{low} melanoma cells (Figure 2b). In addition, a subset of FN1^{high}MITF^{low} melanoma cells displayed strong nuclear ZEB1 immunoreactivity (Figure 2b). Consistent with the gene expression data, we did not observe immunoreactivity for the previously proposed stem-like melanoma cell markers NES and CD133 (data not shown).

FN1 Induction by Hypoxia

The predominant presence of FN1^{high}MITF^{low} melanoma cells in metastatic melanomas with ischemic necrosis suggested a potential role of hypoxia in the induction of these cells. We therefore cultured the A375 melanoma cell line, characterized by low FN1 expression in normoxic conditions (20% O_2 in cell cultures),[23] in hypoxic condition (ie, 1.5% O_2). *FN1* gene expression showed a significant increase by 4.8- and 32-fold after 1 and 3 days of culture in hypoxic conditions when compared with the stable *FN1* expression in control cells cultured at 20% O_2 (Figure 3a). At the protein level, the increase in FN1 expression was clearly apparent at day 3, as shown by immunohistochemistry and western blot analysis (Figure 3a–c). Furthermore, gene expression levels of *HIF2A* and *NGFR* were significantly increased at day 3, whereas expression of *ZEB1*, *ABCB5*, *JARID1B,* and *SNAI1* remained unchanged (Figure 3b). The induction of HIF2A protein was validated by western blot analysis (Figure 3c). Interestingly, ZEB1 displayed a significant increase in protein concentration in hypoxic conditions (but not in mRNA levels), suggestive of a post-transcriptional effect of hypoxia on ZEB1 (Figure 3c). Remarkably, the anti-FN1 antibody revealed not only the conventional FN1 signals with a MW of 220–272 kDa, but also a clear-cut additional band/signal around 72 kDa (Figure 3c). This MW likely corresponds to an oncofetal fibronectin variant termed migration-stimulating factor, which is formed by alternative splicing, resulting in a truncated form with a unique decamer at the C-terminus of the protein.[24] However, this possibility could not be confirmed by immunohistochemistry or western blotting with migration-stimulating factor-specific antibodies (data not shown).

Effect of Hypoxia on Functional Epithelial-to-Mesenchymal Transition Features

Because of the phenotypical epithelial-to-mesenchymal transition and stem-like features of melanoma cells grown in hypoxic conditions, we investigated whether these cells also functionally correspond to the slow-cycling subtype of migratory and invasive melanoma cells, as proposed by the phenotype switch model.[6] Therefore, A375 melanoma cells,

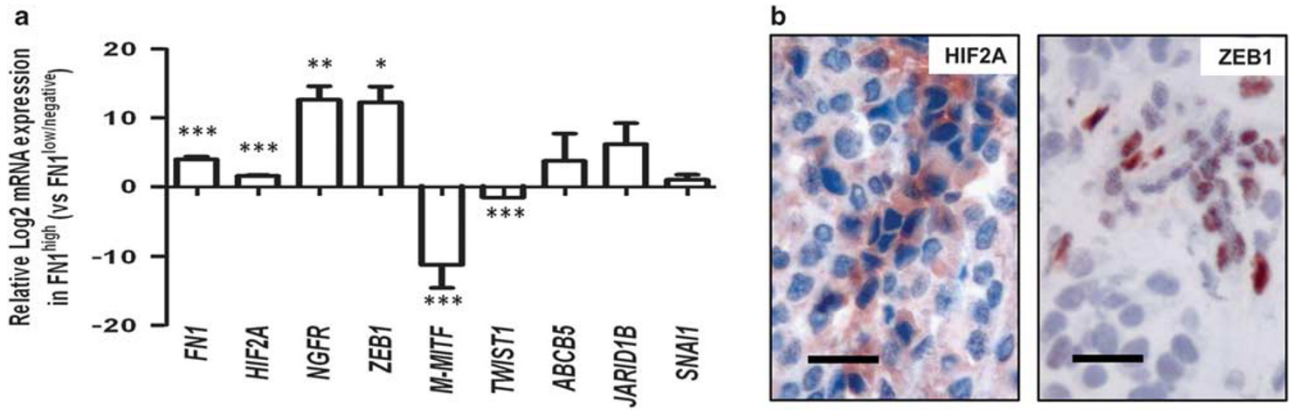

Figure 2 Gene expression analysis of FN1^{high} melanoma cells and validation by immunohistochemistry. (**a**) Gene expression analysis of epithelial-to-mesenchymal transition markers and of previously proposed stem-like melanoma cell markers (see Supplementary Table 1) by RT-qPCR on microdissected FN1^{high} and FN1$^{low/negative}$ melanoma cells ($n=4$; $^{*}P<0.05$; $^{**}P<0.01$; $^{***}P<0.001$; data were statistically analyzed using the two-tailed, one sample *t*-test). (**b**) Immunohistochemical analysis showing expression of HIF2A and ZEB1 (scale bar, 75 μm).

grown in hypoxia for 3 days (when FN1 expression is high; Figure 3), were analyzed for proliferative, migratory, and invasive capacity. Mitotic index was assessed by immunohistochemistry for pHH3[18] and was approximately 3.6-fold lower after 3 days of hypoxia (Figure 4a). In accordance with this observation, the number of cells after 3 days of hypoxia was approximately twofold lower than after 3 days culture in normoxia (Figure 4a). Migratory capacity of near-confluent A375 cells, grown in normoxic/hypoxic conditions for 3 days, was investigated using the wound-healing scratch assay.[20] After 16 h, the migrated surface area was quantified using the TScratch software.[21] The migrated surface area of cells grown in hypoxia was approximately 2.3-fold higher than of cells cultured in normoxic conditions (Figure 4b). Finally, invasive capacity of A375 cells, grown in normoxic/hypoxic conditions for 3 days, was assessed using the ECM-coated Boyden chamber assay.[25] After 24 h, invaded cells were quantified by manual counting and by spectrophotometric analysis. Invasion of cells grown in hypoxia was approximately 1.7- to 10-fold higher than of cells cultured in normoxic conditions (Figure 4c).

Discussion

In the present study, we described a novel melanoma cell type, associated with shortened disease-specific survival, in melanomas that show signs of hypoxia, and provided evidence for their distinct light-microscopic and ultrastructural features, immunohistochemical profile, and gene expression. In routine H&E-stained sections, these FN1^{high}MITF^{low} melanoma cells presented as small, elongated tumor cells with flattened hyperchromatic nucleus. The ultrastructural features of high nucleocytoplasmic ratio, condensed heterochromatin and immature organelles (melanosomes and mitochondria) indicate a poorly differentiated status and suggest a link with stem-like melanoma cells.[26–28] This association is further supported by little or no expression of the melanocytic marker MITF[29] and the unique and high expression of FN1 indicative of an epithelial-to-mesenchymal transition-linked phenotype.[7] Furthermore, gene expression analysis of microdissected FN1^{high} melanoma cells revealed expression of other epithelial-to-mesenchymal transition (*SNAI1* and ZEB1) and previously proposed stem-like melanoma cell markers (*ABCB5*, HIF2A, *JARID1B,* and *NGFR*). Finally, the link with hypoxia was supported by *in vitro* studies, which showed that the cell phenotype was induced by culturing melanoma cells under hypoxic conditions. Within the model of phenotype switching of melanoma cells between a proliferative status and a stem cell-like status with migratory capacities because of epithelial-to-mesenchymal transition, we propose that the FN1^{high}MITF^{low} melanoma cells represent a cell type at the crossroads of stem-like cell induction and epithelial-to-mesenchymal transition.

Although ischemic necrosis is frequently seen in metastatic melanoma and immunohistochemistry for MITF is regularly performed in routine diagnosis of melanocytic lesions, our study is the first to describe the above-mentioned cells. These cells may have been overlooked for the following reasons. First, because they are almost exclusively present in melanocytic lesions with signs of ischemic necrosis, these small, elongated cells with pyknotic nuclei may have been regarded as apoptotic cells. However, their morphology, ultrastructural features, and immunophenotype argue against this possibility. Second, their mesenchymal morphological features and frequent localization close to fibrovascular septa may have caused these cells to be categorized as belonging to the stroma and to correspond to (myo)fibroblasts or endothelial cells. However, we did not detect CD31, CD34, CD144, D2-40, or SMA in the FN1^{high}MITF^{low} melanoma cells. Intriguingly, two other studies detected cells morphologically

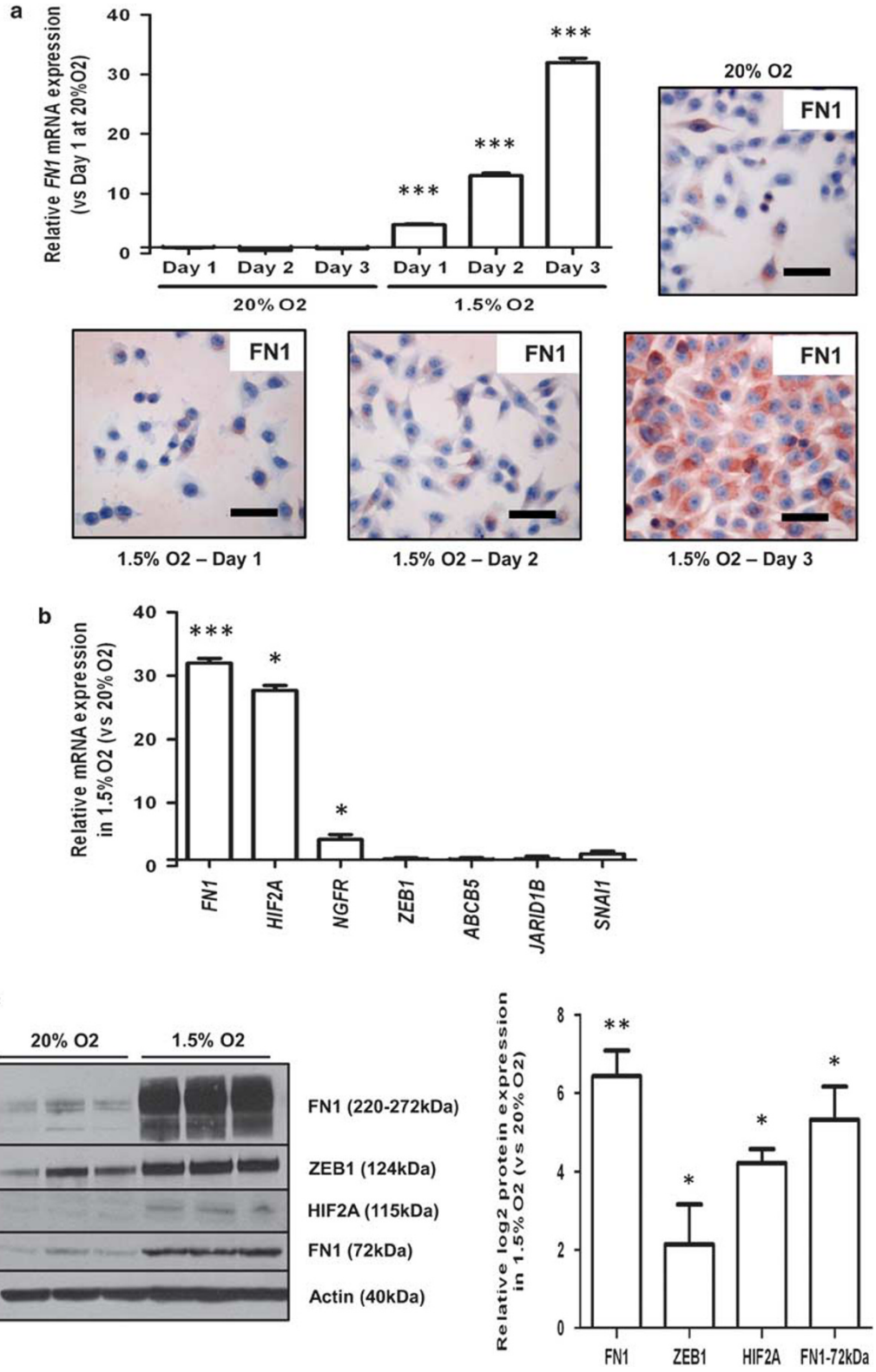

Figure 3 Effect of hypoxia on gene and protein expression in A375 melanoma cells. (**a**) FN1 gene expression in normoxic (20% O_2) and hypoxic (1.5% O_2) conditions after 1–3 days. A375 melanoma cells grown in hypoxia for 1–3 days immunostained for FN1 and normoxic control ($n=3$; $^{***}P<0.001$; scale bar, 150 μm). (**b**) Gene expression analysis of epithelial-to-mesenchymal transition markers and of previously proposed stem-like melanoma cell markers (found upregulated in microdissected FN1^{high} melanoma cells) by RT-qPCR on A375 melanoma cells grown in hypoxia for 3 days ($n=3$; $^{*}P<0.05$; $^{*}P<0.01$; $^{***}P<0.001$). (**c**) Left, western blot analysis of A375 melanoma cells grown in hypoxic conditions for 3 days with antibodies against FN1 (showing bands at 2 heights), ZEB1, HIF2A, and actin (control). Right, quantitative summary of western blots ($n=3$; $^{*}P<0.05$; data in panels **a–c** were statistically analyzed using the two-tailed, one sample *t*-test).

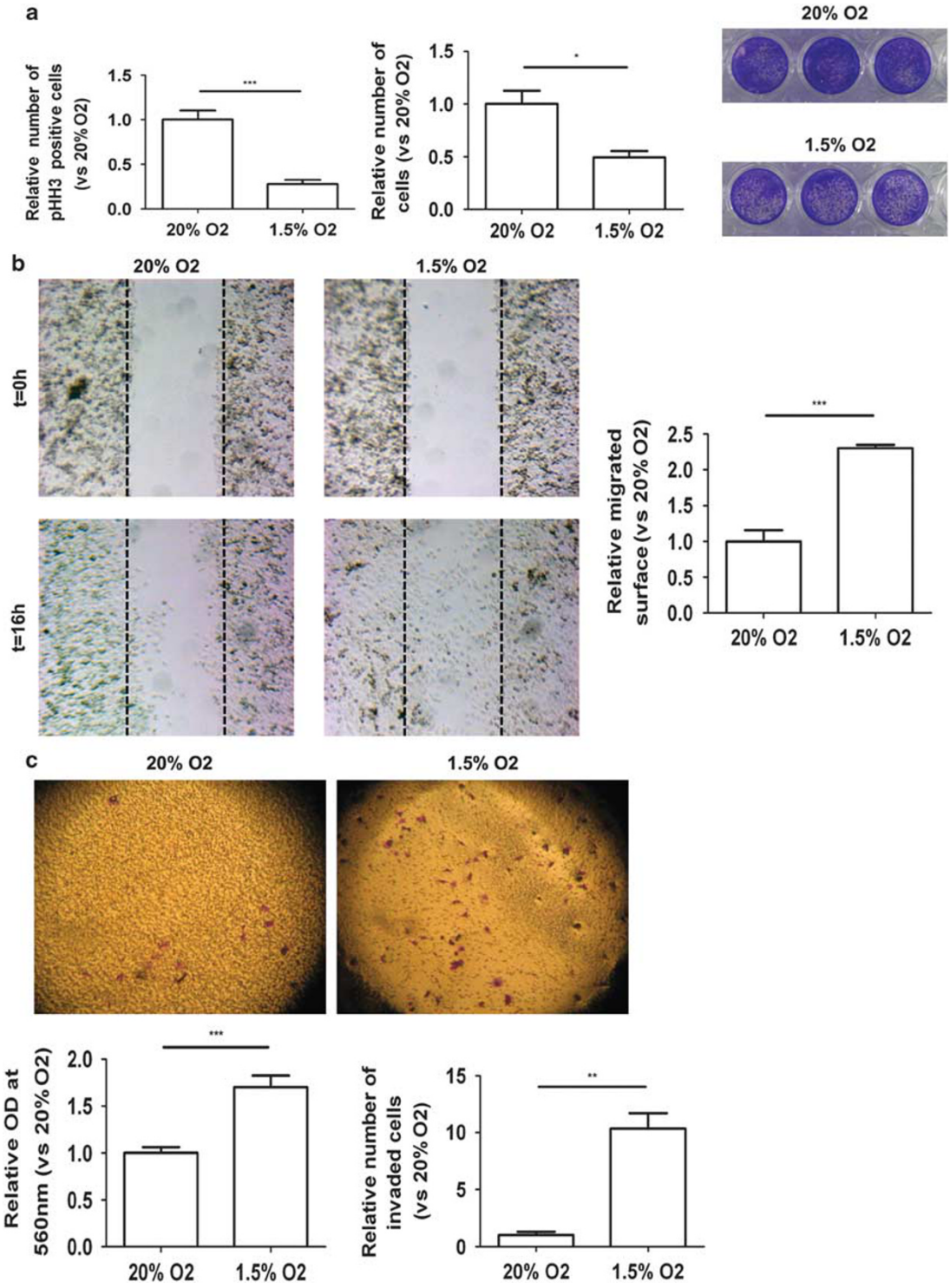

Figure 4 Effect of hypoxia on function of A375 melanoma cells. (**a**) Left, number of pHH3^{positive} A375 melanoma cells after 3 days of culture in normoxic (20% O_2) and hypoxic (1.5% O_2) conditions. Center, number of A375 cells after culturing equal numbers of cells in normoxic and hypoxic conditions (3 days). Right, methylene blue-stained A375 cells after culturing equal numbers of cells in normoxic and hypoxic conditions (3 days; $n=3$; $^{*}P<0.05$; $^{***}P<0.001$). (**b**) Left, wound-healing scratch assays of A375 melanoma cells grown in normoxic/hypoxic conditions for 3 days. Right, quantitative summary of scratch assays (16 h; $n=6$; $^{***}P<0.001$). (**c**) Left, cell invasion assays (ECM-coated Boyden chamber) of A375 melanoma cells grown in normoxic/hypoxic conditions for 3 days. Center, quantitative summary of invasion assays by spectrophotometric analysis. Right, quantitative summary of invasion assays by manually counting invaded cells (24 h; $n=3$; $^{**}P<0.01$; $^{***}P<0.001$; data in panels **a–c** were statistically analyzed using the two-tailed, unpaired Student's *t*-test).

identical to FN1^{high}MITF^{low} cells in ischemic melanomas in experimental animals. These cells were found to be melanocytic in nature but also to express endothelial markers (CD31 and MECA32) and were shown to contribute to neo-angiogenesis.[30,31] Although we did not observe any apparent vessel formation within clusters of the FN1^{high}MITF^{low} cells, we cannot formally eliminate the possibility that these cells contribute to new vessel formation.

FN1^{high}MITF^{low} melanoma cells express high levels of genes that have been associated with stem-like cells and epithelial-to-mesenchymal transition in melanoma or other cancers, and of genes that link epithelial-to-mesenchymal transition and cancer stemness. The hypoxia-inducible factor HIF2A has repeatedly been proposed as a stem-like cell marker in various cancer types, including melanoma.[32–37] In addition, hypoxia and its effector HIF2A have recently been suggested to induce epithelial-to-mesenchymal transition through the inhibition of miRNA-200b and the subsequent induction of *ZEB1*.[38,39] ZEB1 is a well-established epithelial-to-mesenchymal transition inducer in melanoma cells[40] and generally promotes tumorigenicity and stemness.[41] We observed an increase in ZEB1 protein in A375 melanoma cells cultured in hypoxic conditions, although *ZEB1* mRNA levels did not change. This apparent discrepancy may be explained by the hypoxia-induced suppression of miRNA-200b and miRNA-200 family members, which inhibit translation but not transcription of ZEB1 and of which the loss of expression is associated with melanoma progression.[39,42] Other epithelial-to-mesenchymal transition-regulatory transcription factors like SNAI1 and SNAI2 are not expressed in the FN1^{high}MITF^{low} melanoma cells; SNAI1/2 are early epithelial-to-mesenchymal transition markers implicated in the initial induction of a migratory phenotype, whereas ZEB1 is an important regulator of the maintenance of this phenotype.[40,43] MITF was recently proposed as the transcriptional switch that drives stem-like melanoma cells toward differentiation,[29] which is in line with our hypothesis that FN1^{high}MITF^{low} melanoma cells may represent a reservoir of slow-cycling stem-like/tumor-driving cells. Interestingly, hypoxia represses *MITF* expression and thereby enhances the metastatic potential of melanoma cells.[44] Furthermore, it has been suggested that ZEB1 also represses *MITF* expression.[45] FN1^{high}MITF^{low} melanoma cells also express high levels of NGFR, another stem-like melanoma cell marker.[46,47] Moreover, NGFR is a marker of invasiveness in melanoma[48] and identifies migrating cells in other cancers such as glioma showing epithelial-to-mesenchymal transition-like features.[49] The invasive migratory characteristics of FN1^{high}MITF^{low} melanoma cells were furthermore supported by their preferential localization near fibrovascular septa.

Taken together, our study identifies a novel FN1^{high}MITF^{low} melanoma cell type and provides arguments for a (molecular) phenotype closely related to stem-like cell induction and epithelial-to-mesenchymal transition. Given the clinical relevance of FN1^{high}MITF^{low} melanoma cells, additional research should point out whether melanoma patients can profit from adjusted therapy, targeted against FN1, or associated markers. Because FN1^{high}MITF^{low} melanoma cells were identified virtually exclusively in metastatic melanomas with signs of ischemic tumor necrosis, and because hypoxic conditions can *in vitro* induce the phenotype, we propose that hypoxia is an important trigger for the induction of FN1^{high}MITF^{low} melanoma cells.

Acknowledgments

We thank Professor Dr Rita Devos (University of Leuven, KU Leuven) for her help with electron microscopy and all contributing personnel of Translational Cell and Tissue Research (University of Leuven, KU Leuven) for technical assistance.

Research was made possible by funding support from the Fund for Scientific Research-Flanders (Belgium) (FWO-Vlaanderen), the Research Fund (Onderzoeksfonds) of the University of Leuven (KU Leuven), a research scholarship Emmanuel van der Schueren of the Flemish League against Cancer for J.W. (Vlaamse Liga tegen Kanker), and the Cycle For Life Award from the Leuven Cancer Institute (Leuven, Belgium).

Disclosure/conflict of interest

The authors declare no conflict of interest.

References

1 Magro CM, Crowson AN, Mihm MC. Unusual variants of malignant melanoma. Mod Pathol 2006;19 (Suppl 2):S41–S70.
2 Freedman JA, Tyler DS, Nevins JR, *et al.* Use of gene expression and pathway signatures to characterize the complexity of human melanoma. Am J Pathol 2011; 178:2513–2522.
3 Ruiter D, Bogenrieder T, Elder D, *et al.* Melanoma-stroma interactions: structural and functional aspects. Lancet Oncol 2002;3:35–43.
4 Shackleton M, Quintana E, Fearon ER, *et al.* Heterogeneity in cancer: cancer stem cells versus clonal evolution. Cell 2009;138:822–829.
5 Li Y, Laterra J. Cancer stem cells: distinct entities or dynamically regulated phenotypes? Cancer Res 2012; 72:576–580.
6 Hoek KS, Goding CR. Cancer stem cells versus phenotype-switching in melanoma. Pigment Cell Melanoma Res 2010;23:746–759.
7 Thiery JP, Sleeman JP. Complex networks orchestrate epithelial-mesenchymal transitions. Nat Rev Mol Cell Biol 2006;7:131–142.

8 Shirley SH, Greene VR, Duncan LM, *et al.* Slug expression during melanoma progression. Am J Pathol 2012;180:2479–2489.
9 Alonso SR, Tracey L, Ortiz P, *et al.* A high-throughput study in melanoma identifies epithelial-mesenchymal transition as a major determinant of metastasis. Cancer Res 2007;67:3450–3460.
10 Kashani-Sabet M, Venna S, Nosrati M, *et al.* A multi-marker prognostic assay for primary cutaneous melanoma. Clin Cancer Res 2009;15:6987–6992.
11 Haqq C, Nosrati M, Sudilovsky D, *et al.* The gene expression signatures of melanoma progression. Proc Natl Acad Sci USA 2005;102:6092–6097.
12 Jaeger J, Koczan D, Thiesen HJ, *et al.* Gene expression signatures for tumor progression, tumor subtype, and tumor thickness in laser-microdissected melanoma tissues. Clin Cancer Res 2007;13:806–815.
13 Giard DJ, Aaronson SA, Todaro GJ, *et al. In vitro* cultivation of human tumors: establishment of cell lines derived from a series of solid tumors. J Natl Cancer Inst 1973;51:1417–1423.
14 van der Loos CM, van den Oord JJ, Das PK, *et al.* Use of commercially available monoclonal antibodies for immunoenzyme double staining. Histochem J 1988; 20:409–413.
15 Wouters J, Stas M, Govaere O, *et al.* Gene expression changes in melanoma metastases in response to high-dose chemotherapy during isolated limb perfusion. Pigment Cell Melanoma Res 2012;25:454–465.
16 Marshall OJ. PerlPrimer: cross-platform, graphical primer design for standard, bisulphite and real-time PCR. Bioinformatics 2004;20:2471–2472.
17 Schmittgen TD, Livak KJ. Analyzing real-time PCR data by the comparative C(T) method. Nat Protoc 2008; 3:1101–1108.
18 Hans F, Dimitrov S. Histone H3 phosphorylation and cell division. Oncogene 2001;20:3021–3027.
19 Schneider CA, Rasband WS, Eliceiri KW. NIH Image to ImageJ: 25 years of image analysis. Nat Methods 2012;9:671–675.
20 Liang CC, Park AY, Guan JL. *In vitro* scratch assay: a convenient and inexpensive method for analysis of cell migration *in vitro*. Nat Protoc 2007;2:329–333.
21 Geback T, Schulz MM, Koumoutsakos P, *et al.* TScratch: a novel and simple software tool for automated analysis of monolayer wound healing assays. Biotechniques 2009;46:265–274.
22 Raposo G, Marks MS. Melanosomes–dark organelles enlighten endosomal membrane transport. Nat Rev Mol Cell Biol 2007;8:786–797.
23 Gaggioli C, Robert G, Bertolotto C, *et al.* Tumor-derived fibronectin is involved in melanoma cell invasion and regulated by V600E B-Raf signaling pathway. J Invest Dermatol 2007;127:400–410.
24 Schor SL, Ellis IR, Jones SJ, *et al.* Migration-stimulating factor: a genetically truncated onco-fetal fibronectin isoform expressed by carcinoma and tumor-associated stromal cells. Cancer Res 2003;63: 8827–8836.
25 Falasca M, Raimondi C, Maffucci T. Boyden chamber. Methods Mol Biol 2011;769:87–95.
26 Park SH, Kook MC, Kim EY, *et al.* Ultrastructure of human embryonic stem cells and spontaneous and retinoic acid-induced differentiating cells. Ultrastruct Pathol 2004;28:229–238.
27 Mumaw JL, Machacek D, Shields JP, *et al.* Neural differentiation of human embryonic stem cells at the ultrastructural level. Microsc Microanal 2010;16: 80–90.
28 Oh SK, Kim HS, Ahn HJ, *et al.* Derivation and characterization of new human embryonic stem cell lines: SNUhES1, SNUhES2, and SNUhES3. Stem Cells 2005;23:211–219.
29 Cheli Y, Giuliano S, Botton T, *et al.* Mitf is the key molecular switch between mouse or human melanoma initiating cells and their differentiated progeny. Oncogene 2011;30:2307–2318.
30 Mihic-Probst D, Ikenberg K, Tinguely M, *et al.* Tumor cell plasticity and angiogenesis in human melanomas. PLoS ONE 2012;7:e33571.
31 Sun B, Zhang D, Zhang S, *et al.* Hypoxia influences vasculogenic mimicry channel formation and tumor invasion-related protein expression in melanoma. Cancer Lett 2007;249:188–197.
32 Heddleston JM, Li Z, McLendon RE, *et al.* The hypoxic microenvironment maintains glioblastoma stem cells and promotes reprogramming towards a cancer stem cell phenotype. Cell Cycle 2009;8:3274–3284.
33 Holmquist-Mengelbier L, Fredlund E, Lofstedt T, *et al.* Recruitment of HIF-1alpha and HIF-2alpha to common target genes is differentially regulated in neuroblastoma: HIF-2alpha promotes an aggressive phenotype. Cancer Cell 2006;10:413–423.
34 Li Z, Bao S, Wu Q, *et al.* Hypoxia-inducible factors regulate tumorigenic capacity of glioma stem cells. Cancer Cell 2009;15:501–513.
35 Liu S, Kumar SM, Martin JS, *et al.* Snail1 mediates hypoxia-induced melanoma progression. Am J Pathol 2011;179:3020–3031.
36 McCord AM, Jamal M, Shankavaram UT, *et al.* Physiologic oxygen concentration enhances the stem-like properties of CD133+ human glioblastoma cells *in vitro*. Mol Cancer Res 2009;7:489–497.
37 Pietras A, Gisselsson D, Ora I, *et al.* High levels of HIF-2alpha highlight an immature neural crest-like neuroblastoma cell cohort located in a perivascular niche. J Pathol 2008;214:482–488.
38 Xu Y, Li Y, Pang Y, *et al.* EMT and stem cell-like properties associated with HIF-2alpha are involved in arsenite-induced transformation of human bronchial epithelial cells. PLoS ONE 2012;7:e37765.
39 Chan YC, Khanna S, Roy S, *et al.* miR-200b targets Ets-1 and is down-regulated by hypoxia to induce angiogenic response of endothelial cells. J Biol Chem 2011;286:2047–2056.
40 Wels C, Joshi S, Koefinger P, *et al.* Transcriptional activation of ZEB1 by Slug leads to cooperative regulation of the epithelial-mesenchymal transition-like phenotype in melanoma. J Invest Dermatol 2011;131:1877–1885.
41 Wellner U, Schubert J, Burk UC, *et al.* The EMT-activator ZEB1 promotes tumorigenicity by repressing stemness-inhibiting microRNAs. Nat Cell Biol 2009;11:1487–1495.
42 van Kempen LC, van den Hurk K, Lazar V, *et al.* Loss of microRNA-200a and c, and microRNA-203 expression at the invasive front of primary cutaneous melanoma is associated with increased thickness and disease progression. Virchows Arch 2012;461: 441–448.
43 Peinado H, Olmeda D, Cano A. Snail, Zeb and bHLH factors in tumour progression: an alliance against the epithelial phenotype? Nat Rev Cancer 2007;7: 415–428.

44 Feige E, Yokoyama S, Levy C, *et al.* Hypoxia-induced transcriptional repression of the melanoma-associated oncogene MITF. Proc Natl Acad Sci USA 2011;108: E924–E933.
45 Liu Y, Ye F, Li Q, *et al.* Zeb1 represses Mitf and regulates pigment synthesis, cell proliferation, and epithelial morphology. Invest Ophthalmol Vis Sci 2009;50:5080–5088.
46 Boiko AD, Razorenova OV, van de Rijn M, *et al.* Human melanoma-initiating cells express neural crest nerve growth factor receptor CD271. Nature 2010;466:133–137.
47 Civenni G, Walter A, Kobert N, *et al.* Human CD271-positive melanoma stem cells associated with metastasis establish tumor heterogeneity and long-term growth. Cancer Res 2011;71:3098–3109.
48 Chan MM, Tahan SR. Low-affinity nerve growth factor receptor (P75 NGFR) as a marker of perineural invasion in malignant melanomas. J Cutan Pathol 2010;37:336–343.
49 Johnston AL, Lun X, Rahn JJ, *et al.* The p75 neurotrophin receptor is a central regulator of glioma invasion. PLoS Biol 2007;5:e212.

Supplementary Information accompanies the paper on Modern Pathology website (http://www.nature.com/modpathol)